

Radiographic Study of Interaction of Shock and Detonation Waves in a High Explosive

K. N. Panov,¹ V. A. Komrachkov,¹
and I. S. Tselikov¹

UDC 662.215.5

Translated from *Fizika Goreniya i Vzryva*, Vol. 43, No. 3, pp. 132–138, May–June, 2007.
Original article submitted September 13, 2005; revision submitted July 7, 2006.

Collisions of shock and detonation waves in an HMX-based high explosive are experimentally studied with the use of flash radiography. Based on X-ray patterns, specific features of the wave-interaction process are identified, and qualitative differences are found in detonation formation and evolution in an explosive precompressed by a weak shock wave and in an undisturbed explosive.

Key words: shock wave, detonation wave, shock-wave sensitivity, X-ray radiography, HE initiation, detonation excitation, density distribution.

INTRODUCTION

The shock-wave sensitivity of a high explosive (HE) is known to decrease with increasing its initial density: a higher shock-wave pressure is needed for detonation excitation [1]. It is also known that HE desensitizing occurs if the HE is preliminary loaded by shock waves whose amplitude is too low for detonation excitation: the HE becomes less sensitive to the subsequent shock-wave action. This phenomenon was studied experimentally by loading various HEs by a shock wave (SW) with a stepwise profile [2, 3], by considering reflection of the loading SW from a target [4], etc. Loading of an HE sample by a weak SW alters not only its initial density but also its internal structure: possible effects are fragmentation, collapse of voids, changes in crystal defects and their size distribution, etc.

If the HE has enough time to become unloaded prior to repeated loading, for instance, behind an unsteady SW front or if the SW goes out into a “light” layer [5], the shock-wave sensitivity normally increases. Samples recovered after preliminary loading (which have a “damaged” structure) also display an increased sensitivity to repeated loading [6].

X-ray experiments described in [7] were aimed at studying interaction of shock and detonation waves in a TATB-based HE. It is demonstrated that the detonation wave (DW) ceases to propagate into the region of the HE sample compressed by the SW.

The goal of the present work was a radiographic analysis of the changes in shock-wave sensitivity of an HMX-based HE induced by SW–DW interaction, in particular, in the case of detonation propagation into the sample region compressed by the SW. The parameters measured in the experiments were the density distribution in zones covered by the SW and DW and in the region of interaction of these waves.

STATEMENT OF EXPERIMENTS

The experiments were performed in a 2ÉRIDAN-3 pulsed X-ray facility with a soft spectrum of radiation, threshold energy $E_\gamma \approx 0.75$ MeV, and pulse duration $\Delta t \approx 0.2$ μ sec. The image was recorded onto photochromic screens made of europium-activated barium halogenide (Digital Complex for Computer Radiography — DC-CR). Ionization radiation forms a hidden

¹Institute of Experimental Gas Dynamics and Physics of Explosion, Institute of Experimental Physics (VNIIEF), Russian Federal Nuclear Center, Sarov 607190; root@gdd.vniief.ru.

TABLE 1
Actuation Time of the Gauges and Instants of Radiography

Test number	t_1 , μsec	t_2 , μsec	$t_1 - t_2$, μsec	t_γ , μsec	$\Delta t_1 = t_\gamma - t_1$, μsec	$\Delta t_2 = t_\gamma - t_2$, μsec	$X_{\text{fr},1}; X_{\text{fr},2}$, mm	$v_{\text{fr},1}; v_{\text{fr},2}$, km/sec
1	25.64	23.80	1.84	28.60	2.96	4.80	26; 17	8.8; 3.5
2	23.16	22.76	0.40	29.42	6.26	6.66	37; 22	5.9; 3.3
3	28.37	23.78	4.59	32.48	4.11	8.7	17; 28	4.1; 3.2
4	28.42	23.81	4.61	34.90	6.48	11.09	24; 33	3.7; 3.0

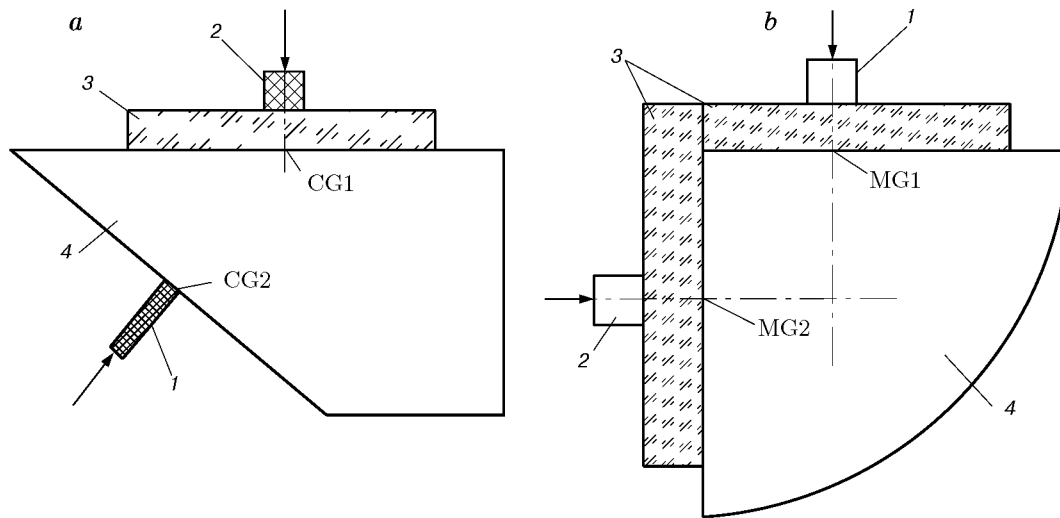


Fig. 1. Layout of the experiment: 1) primer No. 1; cross section 2×10 mm (a) and 8×8 mm (b); 2) primer No. 2 (cross section 8×8 mm); 3) Plexiglas damper; 4) HE sample under study; CG1 and CG2 are the contact gauges; MG1 and MG2 are the manganin gauges.

image in these screens, which can be obtained in digital form by using a special scanner. The photochromic screens have the following characteristics: wide dynamic range of registration (10^4 and more); linear transitional characteristic in a wide range of absorbed doses; single-quantum gamma-sensitivity of the active luminescent material; spatial resolution of ≈ 9 lines/mm or 223 dpi. The use of such screens allows resolving objects with the optical thickness difference of ≈ 0.02 – 0.05 g/cm².

Figure 1 shows the layout of the experimental units. The loading system used in the present experiments was described in [7, 8]. The examined HE sample was initiated by two extended priming charges made of a PETN-based HE through a Plexiglas damper or without the latter. The pressure of the initiating SW was varied by changing the thickness of the damping layer. The primers were actuated at different times, which allowed the SW and DW fronts to collide at different stages of the process. The exact moment of HE loading under each primer was determined on the basis of operation of contact or manganin gauges, which were placed between the damper and the charge.

The sample under study was a pellet whose thickness in the radiography direction was 60 mm. The initial density of the HE samples in all tests was 1.883 g/cm³. The density distribution was determined by the method described in [9]. The essence of the method is determining the density distribution behind the wave front by the formula $\rho(x, y) = Z(x, y)/L_0$, where Z is the optical thickness and L_0 is the initial size of the sample in the direction of X-ray radiography.

TEST RESULTS

In the first test (see Fig. 1a), we considered interaction of a cylindrical DW propagating from the HE surface with an SW that does not transform to detonation (test No. 1). In three subsequent tests, we studied interaction of an SW that does not transform to detonation with a shock wave transforming to detonation at different stages of evolution of the latter.

Table 1 shows the times of SW arrival in the HE under the primers (t_1 and t_2) and the time of X-ray

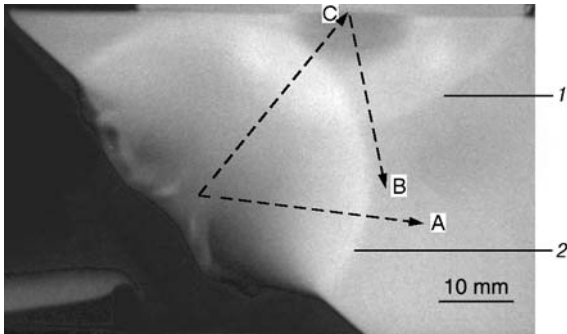


Fig. 2. SW–DW interaction (test No. 1): 1) SW front; 2) DW front; A, B, and C are the directions in which the dependences $\rho(X)$ were determined.

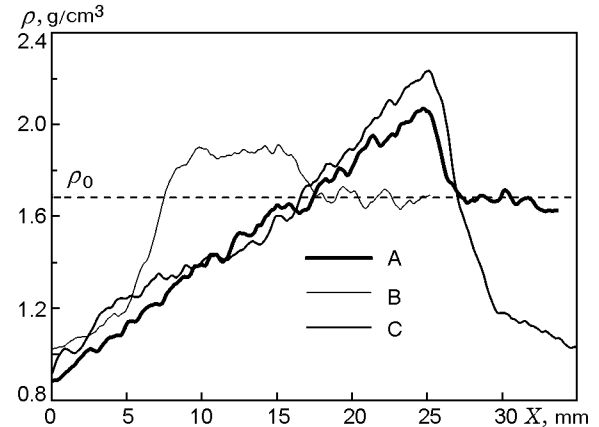


Fig. 3. Density profiles in test No. 1 in the directions indicated in Fig. 2.

radiography (t_γ). Based on the wave-front position X_{fr} measured on the X-ray patterns, we could estimate the mean wave-front velocity in the HE for each primer: $v_{fr,i} = X_{fr,i}/\Delta t_i$.

In test No. 1, the DW was initiated by a PETN-based HE plate 2×10 mm (primer No. 1). The SW was formed by an extended PETN-based priming charges 8×8 mm, which loaded the HE sample through a Plexiglas damper (primer No. 2). The damper thickness in test No. 1 was 10 mm. In this case, an SW with insignificant decomposition of the substance behind the front that does not transform to detonation was formed in the HE.

X-ray radiography of the assembly was performed after SW–DW interaction. Figure 2 shows the X-ray photograph of the explosion process with directions along which the density distribution $\rho(X)$ was determined. It is seen that the DW front passes into the sample region compressed by the SW without distorting its shape, i.e., detonation is not interrupted on the HE compressed by the SW.

Figure 3 shows the density distributions in the directions indicated in Fig. 2. The coordinate $X = 0$ in all plots corresponds to the HE loading surface. The density of the substance behind the SW front is ≈ 2.1 g/cm³ and remains practically unchanged at a distance of ≈ 8 mm behind the front. After that, the density drastically decreases, which is caused by HE decomposition.

It was noted above that there are no visible distortions of the SW and DW front shapes at the moment of X-ray radiography, but the amplitude and density profile in the wave-interaction region differ from both detonation-wave and shock-wave profiles. The density in the wave-interaction region is somewhat higher than that behind the front of the DW propagating over an undisturbed HE.

In test Nos. 2–4 (see Fig. 1b), the colliding waves were an SW that transforms to detonation at a certain depth (primer No. 1) and an SW that did not transform to detonation (primer No. 2). The damper thickness was 8.5 mm under primer No. 1 and 10 mm under primer No. 2. In the first case, a transition of the SW to detonation was observed at a depth of ≈ 12 mm; in the second case, the SW does not transform to detonation. The delay in the actuation time of the primers ($t_1 - t_2$) was varied in the experiments so that the SW encountered the shock-compressed HE at different stages of detonation excitation.

The amplitude of the loading pressure at the SW front measured by manganin gauges was ≈ 4.1 GPa for a 8.5-mm damper and ≈ 3.2 GPa for a 10-mm damper.

Figure 4 shows the X-ray pattern of the explosion process in test No. 2. Detonation is seen to be excited under primer No. 1 at the moment of X-ray radiography. The shape of the DW front suggests that this occurs at a certain depth within a small region near the loading plane. The transition of the SW to the DW is finalized before interaction with the SW front from primer No. 2. The DW front propagates into the compressed region without distortions. A similar pattern was recorded in test No. 1. The results of test Nos. 1 and 2 show that, if the DW is already formed, the compressed HE region located on the DW path does not cause detonation breakdown, as it was registered for a TATB-based HE [7].

The SW front from primer No. 2 changes its shape when entering the region of explosion products. In the zone of the products, it covers a greater distance than in the undisturbed HE region (see Fig. 4). Figure 5 shows the density distributions in the directions indicated in Fig. 4. These dependences clearly show the

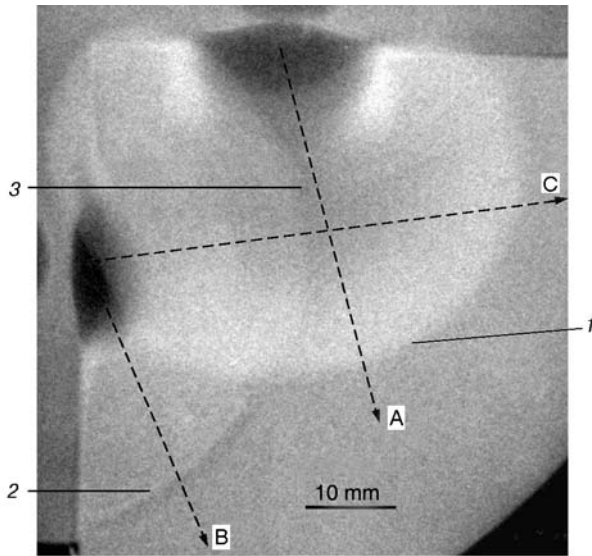


Fig. 4. SW interaction with an SW transforming to detonation (test No. 2): 1) DW front; 2) SW front; 3) SW front in explosion products; A, B, and C are the directions in which the dependences $\rho(X)$ were determined.

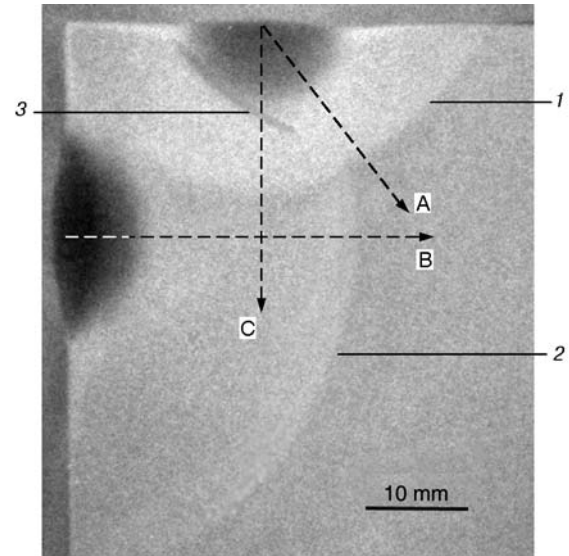


Fig. 6. SW interaction with an SW transforming to detonation (test No. 3): 1) SW front transforming to detonation in an undisturbed HE; 2) SW front; 3) decomposition in the region of interaction of SW fronts; A, B, and C are the directions in which the dependences $\rho(X)$ were determined.

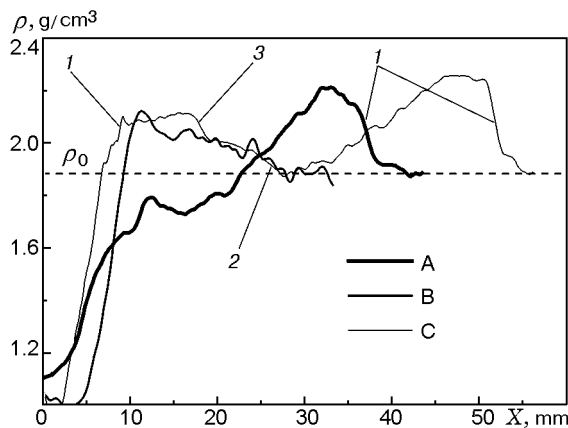


Fig. 5. Density profiles in test No. 2 in the directions indicated in Fig. 4: 1) DW front; 2) SW front; 3) contact boundary (line of collision of the fronts).

difference between the density behavior during SW–DW interaction and the density distribution behind the front of the SW and DW propagating over an undisturbed HE. In addition, the dependence $\rho(X)$ in the direction C clearly displays the characteristic boundaries in the wave-interaction zone.

Figure 6 shows the photograph of the explosion process in test No. 3. In contrast to test No. 2, the SW from primer No. 2 enters the HE $\approx 4.6 \mu\text{sec}$ earlier than the SW from primer No. 1. With a front velocity of $\approx 3 \text{ km/sec}$, the shock wave passes $\approx 14 \text{ mm}$ further

than that in test No. 2. Before transforming to a DW, the SW initiating detonation encounters the substance compressed to a density of $\approx 2.1 \text{ g/cm}^3$. Wave interaction alters the flow parameters behind the SW front, which transforms to detonation in an undisturbed HE. Detonation excitation may fail to occur under these conditions.

X-ray radiography of the assembly was performed $2.15 \mu\text{sec}$ earlier than in test No. 2 (counted from the moment of gauge actuation t_1). It was assumed thereby that the DW under primer No. 1 is to be recorded if preliminary loading by the SW does not affect detonation excitation. It is seen from Fig. 6 that detonation did not occur. In the region where the SW fronts collided, the X-ray pattern shows an extended zone, which is darker than that in the region of the substance compressed behind the front. This may be indicative of HE decomposition at the place of collision of the SW fronts.

Figure 7 shows the density distributions in the directions indicated in Fig. 6. The density behind the SW front under primer No. 2 remains practically unchanged at a distance of $\approx 20 \text{ mm}$ and reaches $\approx 2.0 \text{ g/cm}^3$. The density profiles behind the SW front under primer No. 1 in the undisturbed zone A and in the interaction region C are close to each other. The density of the substance reaches $\approx 2.3 \text{ g/cm}^3$ behind the front and $\approx 2.0 \text{ g/cm}^3$ at the place of collision of the SW fronts.

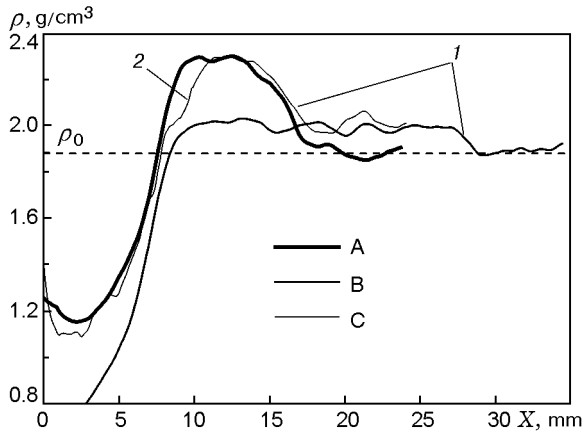


Fig. 7. Density profiles in test No. 3 in the directions indicated in Fig. 6: 1) SW front; 2) zone of HE decomposition due to SW interaction.

In test No. 4, X-ray radiography was performed at a later time to prove that detonation really did not arise. Moreover, it was of interest to see the time evolution of the decomposition zone formed at the place of collision of the SW fronts.

Figure 8 shows the photograph of the explosion process in test No. 4. X-ray radiography was performed $\approx 2.4 \mu\text{sec}$ later than in test No. 3 and $\approx 0.2 \mu\text{sec}$ later than in test No. 2. It is seen from Fig. 8 that detonation did not arise, like in test No. 3. Thus, additional compression of the substance at an earlier stage of the transition to detonation leads to detonation breakdown (cf. Fig. 4 and Fig. 8). As in test No. 3, a zone of HE decomposition at the place of collision of SW fronts was again registered at the same place. Figure 9 shows the density distributions in the directions indicated in Fig. 8. The dependences are in good agreement with data obtained in test No. 3. The density of the substance in the zone of collision of SW fronts is lower and reaches $\approx 1.6 \text{ g/cm}^3$.

DISCUSSION

It is seen from the density distributions that the density of the explosion products behind the front of a cylindrical DW (see Fig. 3) is $\approx 2.3 \text{ g/cm}^3$. The density at the Jouguet point in the approximation of a cubic equation of state of the explosion products is estimated as $\rho_J = (4/3)\rho_0 = 2.5 \text{ g/cm}^3$. The experimental value of density is lower because of DW front smearing. The smearing thickness ΔX depends on several factors. It can be estimated if the DW front velocity $D \approx 8.8 \text{ km/sec}$ and the X-ray pulse duration $\Delta t \approx 0.2 \mu\text{sec}$ are known. Multiplying these two values,

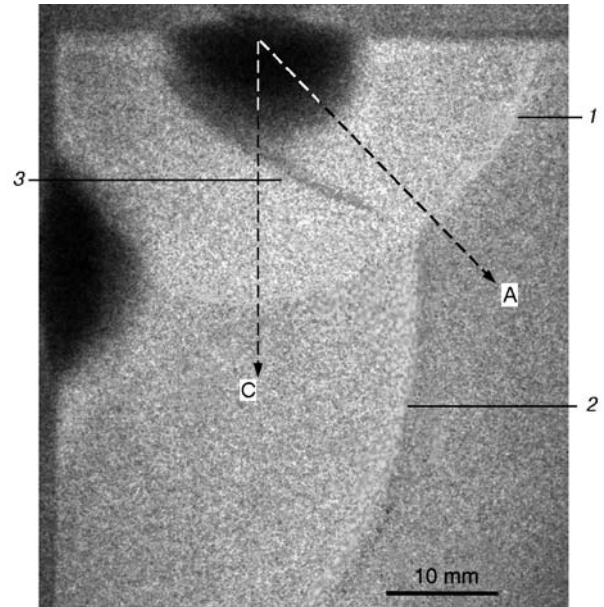


Fig. 8. SW interaction with an SW transforming to detonation (test No. 4): 1) SW front transforming to detonation in an undisturbed HE; 2) SW front; 3) decomposition in the region of interaction of SW fronts; A and C are the directions in which the dependences $\rho(X)$ were determined.

we obtain the smearing thickness $\Delta X \approx 1.8 \text{ mm}$. The experimental value of the DW front smearing thickness is $\Delta X \approx 3 \text{ mm}$. This means that the density cannot be measured at distances smaller than $\Delta X/2 = 1.5 \text{ mm}$ from the DW front. Extrapolation of the experimental distribution of density of the explosion products $\rho(X)$ to the front is difficult because the decrease in density of the products behind the front of the diverging cylindrical DW has a nonlinear character and occurs very fast.

If the SW velocity in the HE is $\approx 3 \text{ km/sec}$, the front smearing thickness is smaller and reaches $\Delta X \approx 1.8 \text{ mm}$, as can be seen from the experimental density profiles. Thus, density measurements at distances smaller than $\approx 1 \text{ mm}$ from the SW front are impossible.

The density of the substance behind the front is determined as the ratio of the optical thickness Z to the initial thickness of the HE sample L_0 in the direction of X-ray radiography. If there is lateral unloading from surfaces perpendicular to the radiography direction, the formula proposed yields an error. The farther from the front, the greater part of the substance along the beam is subjected to unloading. For this reason, the error is systematic and depends both on the distance behind the front and on the distance between the front and the loaded surface. Immediately behind the front, the cal-

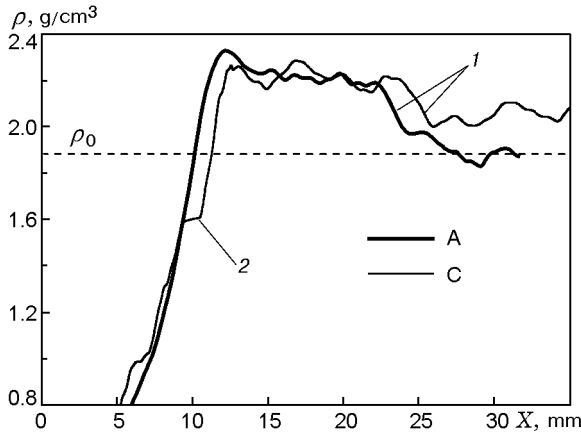


Fig. 9. Density profiles in test No. 4 in the directions indicated in Fig. 8: 1) SW front; 2) zone of HE decomposition due to SW interaction.

culations underpredict the density: the error is negative and stays within $\approx 2\text{--}3\%$. At half of the distance covered by the front, the error becomes close to zero and then positive (in this case, the density is overpredicted). The error reaches a maximum value near the loaded surface and does not exceed $\approx 10\%$ in our case.

It is also necessary to take into account the error in determining the optical thickness Z . This error has a random nature and, being recalculated to density, is smaller than $\approx 2\text{--}3\%$.

The density distributions allow us to quantify the state of the substance in the region of interaction of the SW and DW fronts. Comparing the dependences $\rho(X)$ in the interaction region and behind wave fronts propagating in an undisturbed HE, we can perform a more reliable analysis of the processes inside the HE.

It was experimentally demonstrated that the SW transition to detonation in an HMX-based HE, which occurs under standard conditions, does not occur if the zone of DW formation is precompressed by a weak shock wave to a density of $\approx 2.1\text{ g/cm}^3$. The dependence of shock-wave sensitivity on the initial HE density has been known long ago. In the experiments described, however, we cannot say exactly that precompression of the DW formation zone was the only reason for the absence of detonation excitation. First, a weak SW invokes not only substance densification but also changes in the internal structure of the original HE. Second, after collision of divergent SWs, a complicated flow of the substance is formed, because the mass velocity vector behind the fronts of SWs colliding at different points has different directions. Third, a decrease in density at the place of collision of SW fronts was observed in experiments, which may result from HE decomposition.

The reduced-density zone is located between the region with the products of HE decomposition (dark region in the X-ray patterns) and the front of the SW initiating detonation. A possible consequence is that the SW front becomes devoid of the necessary energy supply from the HE decomposition zone, which is needed for the SW transition to detonation.

It is difficult to tell which of the three factors is mainly responsible for changes in shock-wave sensitivity. It was shown in [7], where similar experiments with a TATB-based HE were performed, that HE compression by a shock wave prevents propagation of the detonation formed into the compressed region. Such an effect is not observed in an HMX-based HE, where the DW front passes to the compressed region almost without any distortions (see test No. 1).

A possible explanation for this phenomenon is the known dependence of shock-wave sensitivity on density. For a TATB-based HE, this dependence is very strong in the range of initial densities $1.89\text{--}1.91\text{ g/cm}^3$ [1]. Moreover, if the substance is compressed to $\approx 2\text{ g/cm}^3$ behind the SW front, the pressure necessary for its initiation exceeds the pressure at the Jouguet point for plasticized TATB. Thus, detonation cannot propagate into the compressed region.

Plasticized HMX does not display such a strong dependence of shock-wave sensitivity on density; in addition, the pressure at the Jouguet point is much higher than that in a TATB-based HE ($p_J \approx 40\text{ GPa}$ and $\approx 29\text{ GPa}$, respectively) [10]. Apparently, this is the reason why the detonation in plasticized HMX can enter the region compressed by the SW.

CONCLUSIONS

The paper describes the experimental results obtained in studying collisions of shock and detonation waves in an HMX-based HE. X-ray patterns make it possible to identify the qualitative differences in detonation formation and evolution in an HE precompressed by a weak shock wave and in an undisturbed HE.

1. The detonation wave propagates into the HE region compressed by the shock wave to a density of $\approx 2.1\text{ g/cm}^3$ without distortions of the front shape and without changes in its velocity.

2. The density of the substance behind the detonation-wave front propagating over a shock-compressed HE is higher than that behind the detonation-wave front in the region of an undisturbed HE.

3. The transition of the shock wave to detonation, which occurs under standard conditions, does not occur if the detonation-wave formation zone is precompressed by a weak shock wave to a density of $\approx 2.1 \text{ g/cm}^3$.

4. A decrease in density of the substance in a narrow zone of collision of shock-wave fronts is registered in experiments.

REFERENCES

1. Yu. A. Vlasov, V. B. Kosolapov, L. V. Fomicheva, and I. P. Khabarov, "Effect of temperature, density, and technical factors on the shock-wave sensitivity of plastic TATB," *Combust., Expl., Shock Waves*, **34**, No. 4, 467–469 (1998).
2. J. K. Dienes and J. D. Kershner, "Multiple-shock initiation via statistical crack mechanics," in: *Proc. 12th Int. Detonation Symp.* (August 11–16, 2002), San Diego (2002).
3. D. A. Salisbury, P. Taylor, R. E. Winter, et al., "Single and double shock initiation of edc37," *ibid.*
4. R. E. Winter, P. Taylor, and D. A. Salisbury, "Reaction of HMX-based explosive caused by regular reflection of shocks," in: *Proc. 11th Int. Detonation Symp.* (August 31–September 4, 1998), Colorado (1998).
5. V. G. Morozov, I. I. Karpenko, S. E. Kuratov, et al., "Theoretical justification of the phenomenological model of shock-wave sensitivity of a heterogeneous TATB-based HE with allowance for single and double loading, including intermediate unloading," *Khim. Fiz.*, **14**, Nos. 2–3, 32–39 (1995).
6. V. A. Komrachkov, A. D. Kovtun, and Yu. M. Makarov, "Increase in shock-wave sensitivity of damaged samples of TATB," *Combust., Expl., Shock Waves*, **35**, No. 4, 436–438 (1999).
7. V. G. Morozov, I. I. Karpenko, V. O. Ol'khov, et al., "Numerical simulations based on experiments with initiation of detonation evolution in TATB-based HE with allowance for desensitizing during interaction of the shock and detonation waves," Preprint, Inst. Exp. Phys., Russian Federal Nuclear Center (1995), pp. 37–95.
8. V. A. Komrachkov, A. D. Kovtun, and Yu. M. Makarov, "Use of pulsed radiography in studies of shock wave initiation of TATB," *Combust., Expl., Shock Waves*, **35**, No. 2, 198–202 (1999).
9. K. N. Panov and V. A. Komrachkov, "Radiographic study of the evolution material of the density profile behind the front of a divergent shock wave in an explosive," *Combust., Expl., Shock Waves*, **40**, No. 5, 591–596 (2004).
10. Ch. Mader, *Numerical Modeling of Detonations*, University of California Press, Berkeley (1983).